Physicochem. Probl. Miner. Process., 62(2), 2026, 220335

http://www.journalssystem.com/ppmp

Physicochemical Problems of Mineral Processing

ISSN 1643-1049

Optimized bioleaching of spent FCC catalysts for the recovery of critical metals

Ceren Erust [1], Mediha Demet Okudan Altındaş [2]

[1] Munzur University Rare Earth Elements Application and Research Center, TR62100, Tunceli, Türkiye

[2] Health Sciences University, Hamidiye Faculty of Health Sciences, Department of Occupational Health and Safety, TR34668, Istanbul, Türkiye

Corresponding author: cerenerust@gmail.com (Ceren Erust)

Abstract: Spent fluid catalytic cracking (FCC) catalysts, generated in large volumes by petroleum refining, represent a promising secondary source of critical metals such as lanthanum, cerium, titanium, and vanadium. In this study, a biohydrometallurgical approach was applied to recover these metals using *Acidithiobacillus ferrooxidans* and *Leptospirillum ferrooxidans*. The spent FCC catalyst, supplied by petroleum refinery, was characterized through WD-XRF, XRD, SEM-EDS, and ICP-OES analyses, confirming significant concentrations of La_2O_3 (1.44%), TiO_2 (1.43%), and CeO_2 (0.23%). Bioleaching experiments were conducted under varying initial ferrous ion concentrations (1–9 g/L) and pulp densities (5–20% w/v) at 35°C over 14 days. Results revealed that the optimal conditions for maximum recovery occurred at 5 g/L Fe^{2+} and 10% pulp density, achieving leaching efficiencies of 95.5% for La, 90.5% for Ce, 92.5% for Ti, and 60.8% for V within seven days. Beyond this period, efficiency decreased due to jarosite formation and microbial activity constraints. The findings confirm that bioleaching is a cost-effective and sustainable route that aligns with circular economy principles by reducing reliance on virgin rare earth mining while mitigating the environmental impact of catalyst disposal.

Keywords: biohydrometallurgy, cerium, critical metals, lanthanum, spent fluid catalytic cracking catalysts

1. Introduction

Fluid catalytic cracking (FCC) catalysts play a critical role in the petroleum refining industry, facilitating the conversion of heavy hydrocarbons into lighter, more valuable fractions such as gasoline and olefins (Akhtar et al., 2024). These catalysts, typically composed of zeolites supported on silica-alumina matrices, are periodically replaced due to deactivation caused by contaminants and structural degradation (Suganuma and Katada, 2020). The annual production of spent FCC catalyst (also referred to as ECAT) is estimated at 700,000–900 tons (Ferella et al., 2016; 2019). As a result, vast quantities of spent FCC catalysts are produced annually, posing both environmental challenges and resource recovery opportunities.

Spent FCC catalysts contain several valuable components, including critical raw materials that are increasingly important for the global economy and the advancement of sustainable technologies. The European Union, along with countries such as the United States and Japan, classify rare earth elements (REEs), titanium, and vanadium as "critical" or "strategic" resources (Kannan et al., 2025). Among the REEs, lanthanum (La) and cerium (Ce) are most frequently incorporated into catalysts to improve their performance and durability. Given the growing demand for REEs in clean energy technologies, electronics, and advanced materials and the geopolitical and environmental issues associated with primary REE mining recovering these elements from secondary sources has become increasingly important.

Hydrometallurgical methods represent an effective approach for reclaiming critical metals from spent FCC catalysts. These processes generally rely on techniques such as leaching, precipitation, solvent extraction, and ion exchange (Li et al., 2011). This approach not only aligns with circular

DOI: 10.37190/ppmp/220335

economy principles by reclaiming critical metals from industrial waste, but also reduces the need for virgin REE extraction. Traditionally, the solubilization of metals from low-grade ores and wastes has relied on chemical leaching with strong inorganic acids such as hydrochloric acid (HCl), sulfuric acid (H_2SO_4), and nitric acid (HNO_3). These acids are effective due to their high leaching efficiency; however, they also demand high energy input and pose serious environmental hazards. As a result, organic acid leaching has emerged as a more environmentally benign alternative. However, synthetic organic acids are generally more expensive than inorganic acids, making their large-scale application less economically viable.

A more environmentally friendly method for metal extraction is bioleaching. This process is widely used for treating low-grade ores and metal-containing waste, as it offers a cost-effective, efficient, and sustainable alternative to traditional methods (Akcil et al., 2015; Santhiya et al., 2006). In particular, studies on the recovery of critical metals from spent FCC catalysts by bioleaching method are attracting attention (Table 1). Aluminium, nickel, titanium, vanadium, and especially lanthanum and cerium are essential elements for bioleaching of spent catalysts (Srichandan et al., 2019).

Table 1. The bioleaching studies on recovering critical metals from spent FCC catalysts

Bacteria	**Experimental Conditions**	**Recovered Metals / Efficiency**	**Reference**
Acidithiobacillus ferrooxidans	Initial Fe(II) 8.84 g/L, 1% pulp density, pH 2.0 ± 0.2, 30 °C, 130 rpm, 10 days	83% La, 23% Ce	Muddanna & Baral (2021)
Acidithiobacillus ferrooxidans	Initial Fe(II) 8.84 g/L, 1% pulp density, pH 2.0 ± 0.1, 10 days	35% Al, 14% Ti, 27% Ni, 56.5% V	Mouna et al. (2021)
Acidithiobacillus caldus	10% (v/v) inoculum, supplemented with 2% (w/v) sulfur pellets, 35–40 °C, 150 rpm, 5 days in polypropylene bioreactor	19.4% Ni, 22.1% V, 53.8% La, 59.6% Ce	Wang et al. (2023)
Acidithiobacillus thiooxidans, *Acidithiobacillus ferrooxidans*, *Leptospirillum ferriphilum*	50 g/L $FeSO_4 \cdot 7H_2O$, 5.6% pulp density, 58 °C, 8 h	49% La, 47% Ce, 9% Al, 8% V (80% regeneration)	Zhang & Xin (2025)
Fungus	**Experimental Conditions**	**Recovered Metals / Efficiency**	**Reference**
Aspergillus niger	Highly Ni-contaminated sample (2600 mg/kg), 5 g/L pulp density, 30 °C, 150 rpm, 21 days	32% Ni	Bayraktar (2005)
Aspergillus niger	1% pulp density, 100 g/L sucrose, 30 °C, 120 rpm, 14 days water bath incubation	9% Ni, 23% Fe, 30% Al, 36% V, 64% Sb	Aung & Ting (2005)
Aspergillus niger, *Aspergillus foetidus*, *Aspergillus carbonarius*	0.8% (w/v) pulp density, 40 g/L sugar as carbon source, 30 °C, 120 rpm, 6 days	88.4% Al	Das et al. (2019)
Aspergillus niger	1% pulp density, 30 °C, 130 rpm, 30 days incubation	50% Al, 32% Ti, 42% V	Muddanna & Baral (2019)

Bayraktar (2005) explored nickel removal from equilibrium FCC catalysts using *Aspergillus niger* and found that bioleaching extracted about 32% of nickel, compared to 21% obtained with citric acid leaching. The improved efficiency was linked to the combined action of fungal mycelium and the localized accumulation of citric acid on the catalyst surface, which also contributed to lowering coke yield and hydrogen-to-methane ratios during cracking. In the same year, Aung and Ting (2005) showed that *Aspergillus niger* was capable of solubilizing several metals, including Ni, Fe, Al, V, and Sb, from spent FCC catalysts, with bioleaching outperforming chemical leaching, especially under conditions of low pulp density.

Das et al. (2019) investigated aluminium recovery from spent FCC catalysts through *Aspergillus niger* bioleaching and reported a maximum leaching efficiency of 88.43% at 0.8% pulp density under optimized conditions. In a related study, Muddanna and Baral (2019) compared bioleaching with chemical leaching of spent FCC catalyst, finding that *Aspergillus niger* achieved high recovery rates of Al (97%), Ti (95%), V (91%), and Fe (94%) at 1% pulp density, whereas nickel showed the best extraction efficiency (82%) with 1 M oxalic acid. These results highlight that bioleaching with *Aspergillus niger*, largely attributed to citric acid secretion, provides a more sustainable and effective approach for metal recovery from spent FCC catalyst than conventional acid leaching.

Mudanna and Baral investigated the recovery of rare earth elements (REEs) from spent fluid catalytic cracking catalyst (SFCCC) using *Acidithiobacillus ferrooxidans*, achieving maximum leaching efficiencies of up to 71% La, 69% Ce, and 65% Nd at 1% pulp density under optimized conditions. Compared to the *Aspergillus niger* bioleaching process, which achieved 88.43% Al recovery at 0.8% pulp density, this study highlights the applicability of the bioleaching process for different target elements; however, fungal leaching was more efficient for aluminium, while bacterial systems were more effective for REEs. While Mudanna and Baral (2021) achieved the leaching of rare earth elements, the maximum leaching efficiency reached 28% Al, 5% Ti, 16.5% Ni and 29% V in the study by Mouna et al. (2021) with *Acidithiobacillus ferrooxidans* under the same initial iron concentration (8.84 g/L Fe (II)) and pulp density (1%). Reed and colleagues (2016) investigated the bioleaching of vanadium and nickel from spent petroleum catalyst using *Acidithiobacillus ferrooxidans*, achieving solubilization efficiencies of up to 95% V and 60% Ni under optimized conditions.

Wang and his colleagues (2023) developed an adapted strain of *Acidithiobacillus caldus* UVS10 that effectively bioleached Ni (19.4%), V (22.1%), La (53.8%), and Ce (59.6%) from spent fluid catalytic cracking catalysts, with bioreactor experiments. Zhang and Xin (2025) developed a rapid and eco-friendly regeneration method for spent FCC catalysts using an indirect bioleaching 'spent medium process,' which selectively removed metals such as Ni, Fe, and V within just 8 hours. Under optimized conditions (58°C, 5.6% pulp density), the regenerated catalysts recovered up to 80% of their original activity, significantly outperforming mixed acid treatment, and demonstrated improved surface area and pore structure. Therefore, the dual-species system was selected to maintain a more robust Fe^{2+} oxidation cycle and acidic leaching environment than could typically be expected from a single-species culture. Bioleaching represents a promising approach not only for the recovery of critical metals but also for the regeneration of spent catalysts.

This article presents the biohydrometallurgical experimental procedure for the efficient recovery of Ni, Ti, V, La and Ce from spent FCC catalysts. The applied experimental procedure is shown in Figure 1 and consists of the following steps.

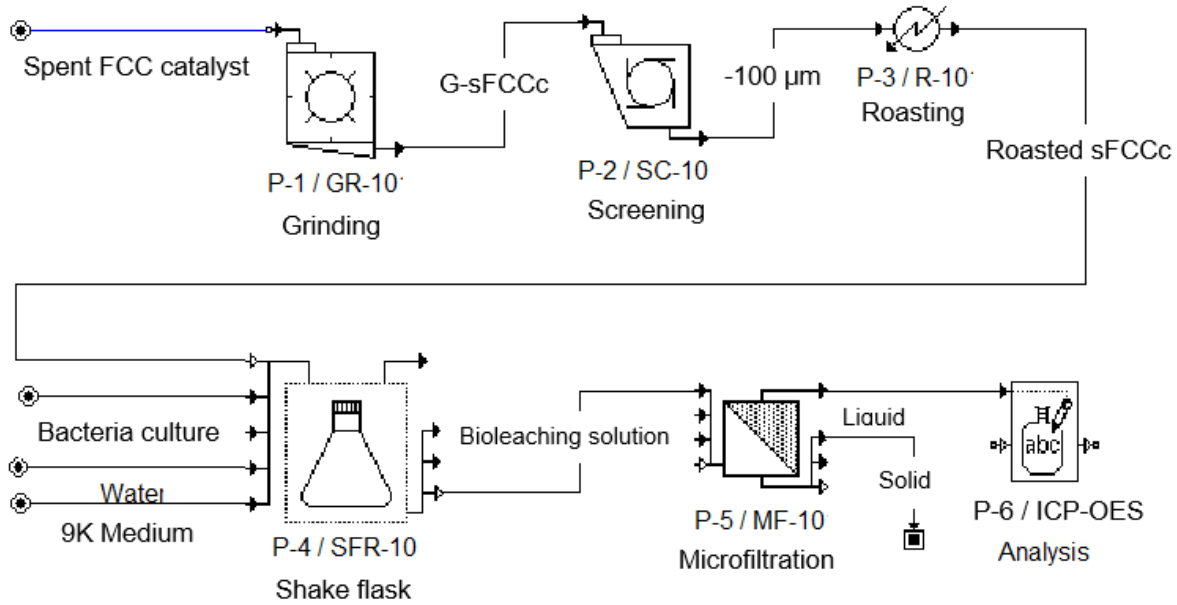

Fig. 1. Flowsheet of bioleaching on spent fluid catalytic cracking catalyst

2. Materials and methods

2.1. Material

The spent FCC catalyst (ECAT) was provided by petroleum refinery, which was used as the base material in all bioleaching experiments. The spent FCC catalysts were systematically ground and screened for size reduction. The sample was ground with a planetary mill (Fritsch Pulverisette 5/2) and screened to -100 μm size with ASTM E-11 type test sieves.

2.2. Characteristics of spent FCC catalysts

Elemental analysis of the spent FCC catalysts was performed using wavelength-dispersive X-ray fluorescence (WD-XRF, Malvern Panalytical Zetium). Measurements were conducted at 20 kV with acquisition conditions of 0° tilt, 0° azimuth, 30° elevation, and a 30° effective take-off angle, repeated in three iterations to ensure reproducibility. X-ray diffraction (XRD) patterns were obtained using a Rigaku Miniflex600 diffractometer within a 2θ range of 5–50°. The instrument was operated at 40 kV and 10 mA with CuKα radiation, using a continuous scanning speed of 5°/min.

The surface morphology and elemental distribution of the spent FCC catalysts were characterized by scanning electron microscopy (SEM, Hitachi SU3500) coupled with energy-dispersive X-ray spectroscopy (EDX, Oxford INCA). For metal content determination in the bioleaching solutions, inductively coupled plasma–optical emission spectrometry (ICP-OES, Thermo Fisher Scientific, iCAP Pro XP Duo) was employed. Prior to ICP-OES analysis, the leachate solutions were filtered through 0.45 μm MF-Millipore membranes to prevent clogging of instrument capillaries.

2.3. Bioleaching

The bioleaching strains *Acidithiobacillus ferrooxidans* (DSM 14882) and *Leptospirillum ferrooxidans* (DSM 2705) were obtained from the German Collection of Microorganisms and Cell Cultures GmbH (DSMZ, Germany). The consortium was designed based on the complementary iron-oxidizing capabilities of the two acidophiles, with the aim of sustaining ferric iron regeneration and improving leaching stability under relatively high pulp density conditions. Both cultures were activated and introduced into 9K medium with the following chemical composition: $FeSO_4.7H_2O$ (9.0 g/L), $(NH_4)_2SO_3$ (3.0 g/L), $MgSO_4.7H_2O$ (0.5 g/L), KH_2PO_4 (0.5 g/L), Ca $(NO_3)_2.4H_2O$ (0.1 g/L), prepared according to the formulation described by Silverman and Lundgren (1959). Each bioleaching experiment was initiated with a 10% (v/v) inoculum of *Acidithiobacillus ferrooxidans* and *Leptospirillum ferrooxidans* precultures, corresponding to an initial cell density of approximately 1.2×10^8 cells mL^{-1}. All experiments were performed in 250 mL Erlenmeyer flasks with a working volume of 100 mL, incubated in a Jeiotech IST-4075 orbital shaker at 35 °C for 14 days. Bioleaching trials were conducted under varying operating conditions, including initial ferrous ion (Fe^{2+}) concentrations of 1, 3, 5, 7, and 9 g/L, and pulp densities of 5, 10, 15, and 20% (w/v). The pH was adjusted to 2.0 using H_2SO_4. pH and oxidation–reduction potential (ORP) was monitored using a Thermo Scientific Orion Star A215 meter. Redox potential (Oxidation–reduction potential, ORP) was measured with an Ag/AgCl (3 M KCl) reference. Readings were converted to Eh (vs. Standard Hydrogen Electrode, SHE) using +0.217 V at 35 °C (from Ag/AgCl to SHE) and verified daily with Zobell's and Light's solutions (±2 mV criterion). Raw meter readings were therefore relative to Ag/AgCl. The Eq. 1 was applied to report the standard redox potential (Eh) relative to SHE.

$$E_h(\text{vs SHE}) = E_{meas}(\text{vs Ag/AgCl}) + \Delta E_{Ag/AgCl} \quad (1)$$

At 25 °C, ΔE in 3 M KCl is approximately SHE+0.210V. The junction potential was adjusted for temperature using the temperature coefficient of operation (≈ +0.73 mV $°C^{-1}$). Thus, at 35 °C:

$$\Delta E_{Ag/AgCl} = \text{SHE}(35°C) = 0.210V + (10°C \times 0.00073V) = 0.217V \quad (2)$$

The potential difference between Ag/AgCl and SHE at 35 °C is about 0.217 volts. All ORP data in the revision are converted and reported as E_h (V vs. SHE) at the measured solution temperature (35 °C). Ferrous (Fe^{2+}, Fe(II)) and ferric (Fe^{3+}, Fe(III)) concentrations were quantified using a UV–VIS–NIR spectrophotometer (Agilent Technologies Cary 5000).

3. Results and discussion

3.1. Characteristics of spent FCC catalysts

Table 2 summarizes the elemental composition of the spent FCC catalyst obtained from WD-XRF analysis. The dominant oxides were Al_2O_3 and SiO_2, while minor but significant fractions of critical and rare earth oxides were also detected, including La_2O_3 (1.44 wt%), CeO_2 (0.23 wt%), TiO_2 (1.43 wt%), and V_2O_5 (0.74 wt%). Other elements (e.g., Ca, Cr, K, Zn and Ni) with amounts less than 0.1% are not listed in the table.

Table 2. WD-XRF analysis of the spent FCC catalyst

Element	**Al_2O_3**	**SiO_2**	**La_2O_3**	**TiO_2**	**Fe_2O_3**	**V_2O_5**
FCC catalyst (%)	43.09	50.04	**1.44**	**1.43**	1.04	**0.74**
Element	MgO	SO_3	Na_2O	P_2O_5	**CeO_2**	Other
FCC catalyst (%)	0.56	0.35	0.33	0.30	**0.23**	0.45

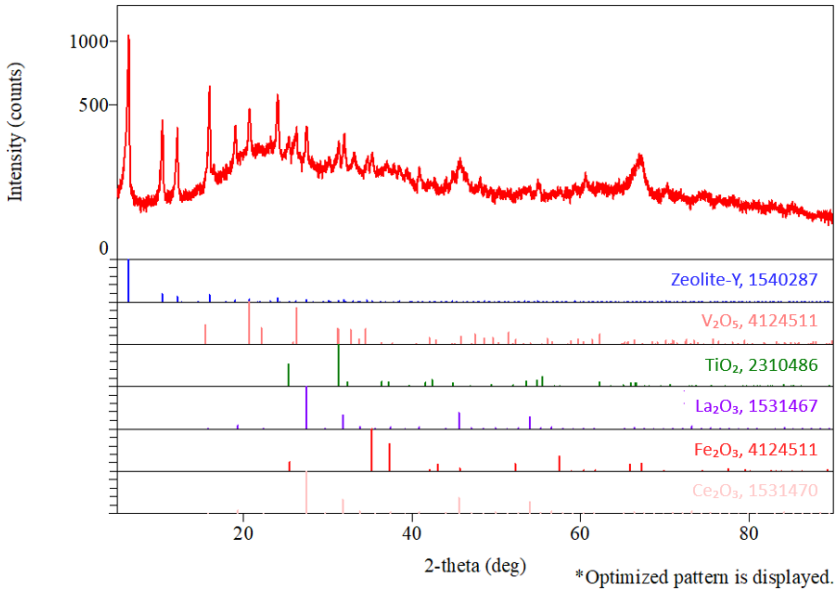

Fig. 2. XRD analysis of the spent FCC catalyst

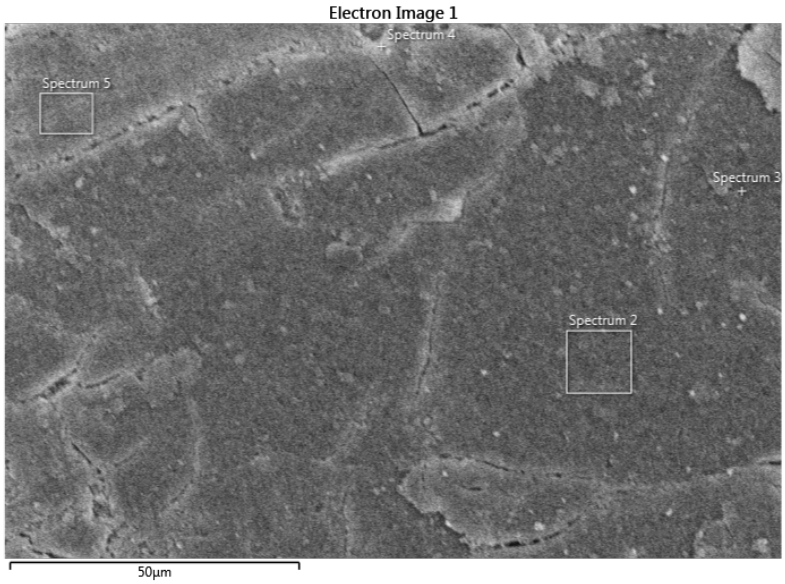

Fig. 3. SEM of the spent FCC catalyst surface morphology (15.0kV, 500 x)

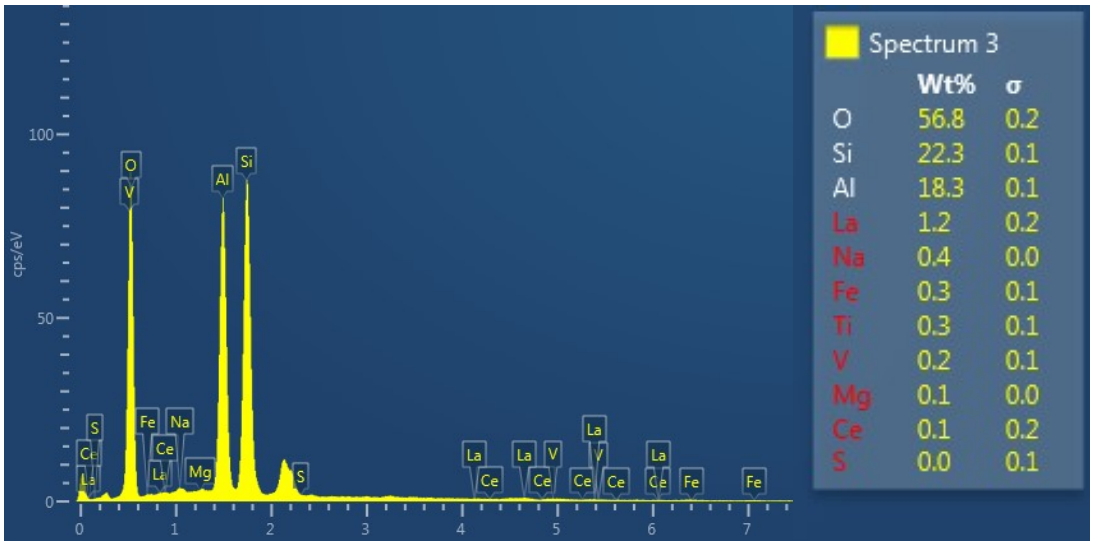

Fig. 4. EDS analysis of the spent FCC catalyst

Fig. 2 presents the XRD profile of zeolite Y (DB card no. 1540287). Distinct diffraction peaks characteristic of zeolite Y are visible at approximately 2θ values of 6°, 10°, 12°, 16°, 19°, and 20°. Although the majority of them are zeolite Y, V_2O_5 (DB card number, 4124511), TiO_2 (DB card number, 2310486), La_2O_3 (DB card number, 1531467), Fe_2O_3 (DB card number, 1532120) and Ce_2O_3 (DB card number, 1531470) peaks are also seen in Figure 2. The surface analysis revealed that the spent catalyst exhibited a rough morphology with sporadic cracking (Fig. 3). The EDS analyses of different point and area spectra were also performed and it is seen that the point-scan analysis results in Figure 4, presented as an example, support the WD-XRF results.

3.2. Bioleaching

3.2.1. Effect of initial ferrous concentration

Quantification of Fe^{2+} and Fe^{3+} ions during the bioleaching process are among the parameters that directly affect the leaching efficiency and gives an idea about the leaching duration (Mousavi et al., 2008). Figs. 5-11 represent the efficiencies of metals between 1 and 9 g/L initial Fe^{2+} concentration in the 10% pulp density (PD). At initial Fe^{2+} concentrations of 1 and 3 g/L, a slight decline in Fe^{2+} levels was observed over the leaching period. At initial Fe^{2+} concentrations of 1 and 3 g/L, bioleaching efficiency did not exceed 75.5% for La, 45.4% for Ce, 35.5% for Ti and 15.6% for V.

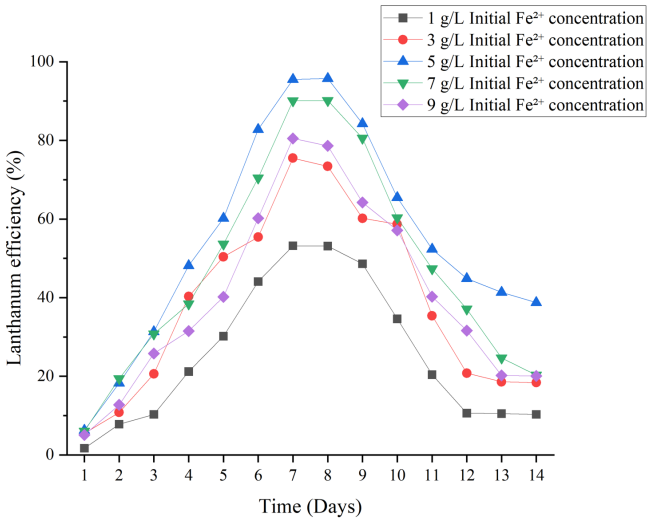

Fig. 5. Lanthanum bioleaching efficiency (%) by *Acidithiobacillus ferrooxidans* and *Leptospirillum ferrooxidans* at 1–9 g/L initial Fe^{2+} concentrations

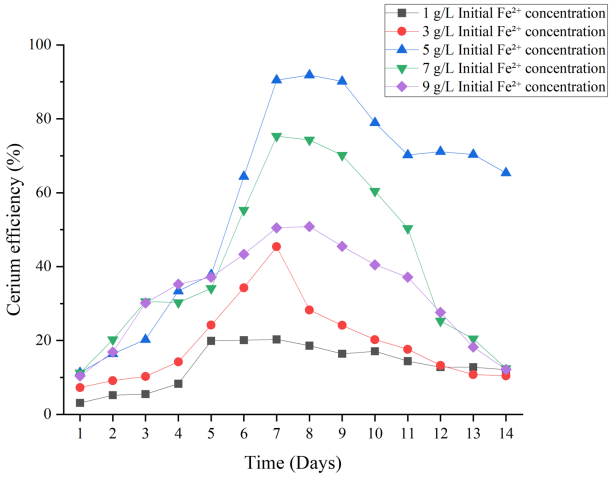

Fig. 6. Cerium bioleaching efficiency (%) by *Acidithiobacillus ferrooxidans* and *Leptospirillum ferrooxidans* at 1–9 g/L initial Fe^{2+} concentrations

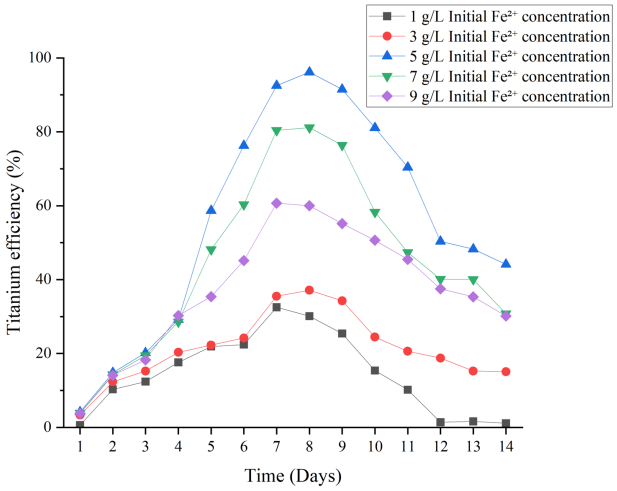

Fig. 7. Titanium bioleaching efficiency (%) by *Acidithiobacillus ferrooxidans* and *Leptospirillum ferrooxidans* at 1–9 g/L initial Fe^{2+} concentrations

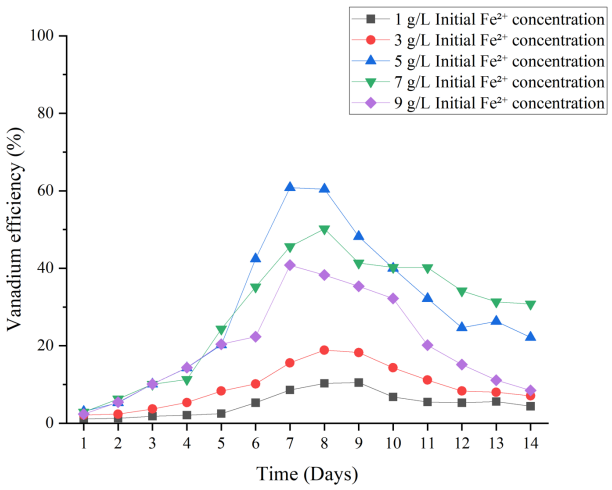

Fig 8. Vanadium bioleaching efficiency (%) by *Acidithiobacillus ferrooxidans* and *Leptospirillum ferrooxidans* at 1–9 g/L initial Fe^{2+} concentrations

Initial Fe^{2+} concentration was high (> 5 g/L) until the day five and by 7 days it approached zero. It is observed that the leaching efficiencies of La, Ce, Ti and V increase gradually in the first 5 days and the leaching efficiency increases rapidly on the 6th and 7th days. The highest bioleaching efficiencies were observed as 95.5% La, 90.5% Ce, 92.5% titanium and 60.8% vanadium on the 7th day at 5 g/L initial Fe^{2+} concentration. Considering that TiO_2 has very low solubility at pH ≈ 2 and 35 °C, which could lead to the presence of colloidal or suspended Ti-containing particles in the bioleaching solution, the bioleaching solutions were reanalysed after removing colloidal phases by 0.02 µm membrane filtration before Ti analysis by ICP-OES. The corrected Ti concentrations showed no significant deviation (<1.5%) from the initially reported values, confirming that colloidal interference was negligible under our experimental conditions.

This indicates that at initial Fe^{2+} concentrations of 7 and 9 g/L, the amount generated exceeded what was required for metal leaching, and the concentrations shown in Fig. 9 represent the residual Fe^{2+} that remained unutilized during the process. After day 7, the leaching efficiency exhibited a marked slowdown and, in some cases, a slight decrease. This behavior can be associated with the precipitation of jarosite due to the participation of Fe^{2+} ions in secondary mineral formation. Jarosite, an insoluble iron-bearing phase, is known to form particularly when the pH exceeds 1.5 and/or the Fe^{2+} concentration in the leaching medium becomes sufficiently high (Daoud and Karamanev, 2006). In order to verify this assumption, XRD analysis was performed from solid residues formed on the edges of the Erlenmeyer flask, and the diffraction patterns clearly revealed the presence of jarosite peaks (Figure 9). In addition, the intensity of these peaks increased with increasing pH, suggesting that jarosite formation was promoted at higher pH values. The formation of this precipitate may have hindered the leaching process by creating a passivating layer on the particle surfaces.

Redox potential (ORP) plays a critical role in the dissolution of metal compounds, as higher ORP values are associated with faster oxidation kinetics (Nagar et al., 2021). According to the Nernst equation (Eq. 3 and 4) (Boon and Heijnen, 1998; Peng et al., 2009), the redox potential is largely dictated by the Fe^{3+}/Fe^{2+} equilibrium (Fig. 12). This relationship was also apparent in the bioleaching experiments, where the small intersection angle between ORP and Fe^{2+} concentrations highlight the strong dependence of redox potential on the Fe^{2+} pool (Figs. 10 and 12).

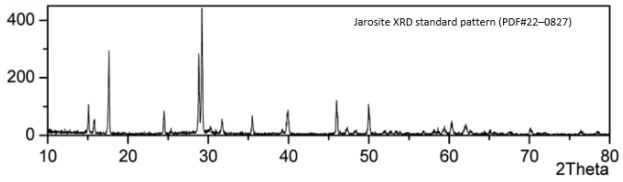

Fig. 9. XRD patterns of the solid residues formed on the edges of the Erlenmeyer flask, showing the formation of jarosite phases

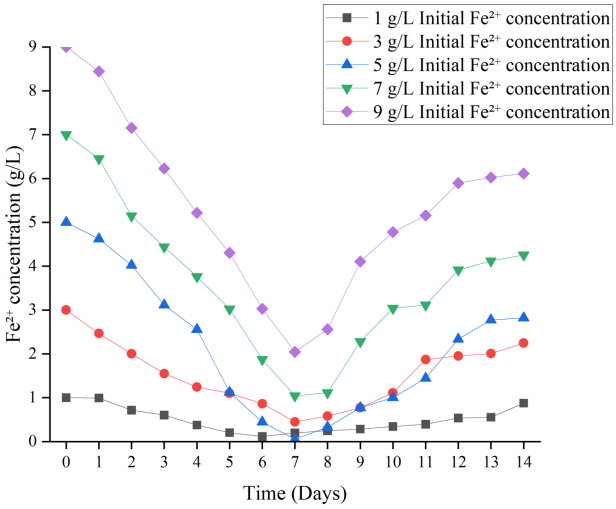

Fig 10. Daily amount of Fe^{2+} consumed by acidophilic bacteria

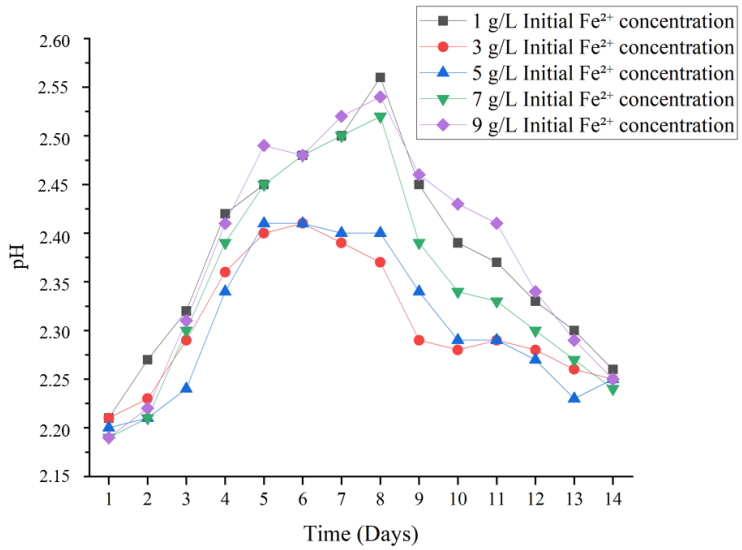

Fig 11. pH variation during the bioleaching at different concentrations of Fe^{2+} concentrations

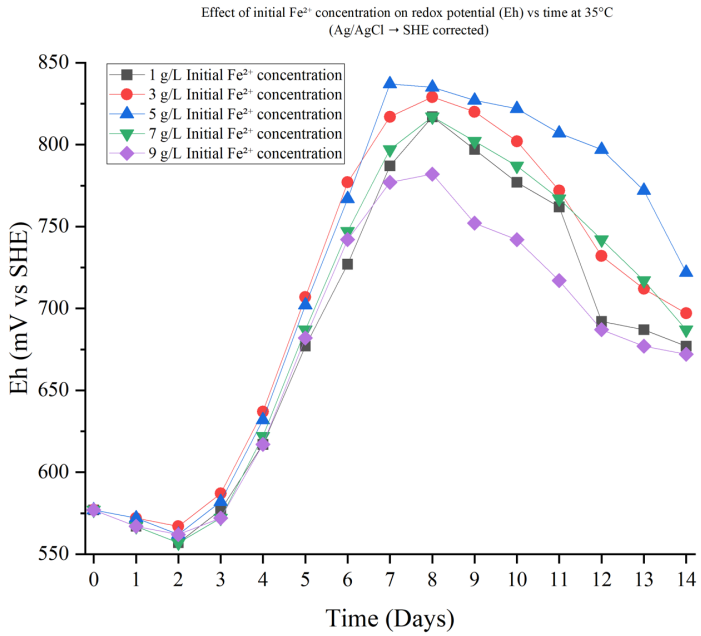

Fig 12. Effect of initial Fe^{2+} concentration on redox potential (Eh) during bioleaching at 35°C

Incomplete oxidation of Fe^{2+} resulted in a lower Fe^{3+}/Fe^{2+} ratio and, consequently, reduced redox potential. This condition may arise from several factors: (i) limited activity or insufficient population density of Fe^{2+}-oxidizing bacteria such as *Acidithiobacillus ferrooxidans* and *Leptospirillum ferrooxidans*, (ii) restricted oxygen availability in the leaching medium, which slows microbial oxidation, or (iii) side reactions such as jarosite precipitation, which consume ferric ions and suppress further redox cycling. The observed leaching behavior, together with the Fe^{2+} consumption profile and Eh evolution, suggests functional complementarity between the two iron-oxidizing microorganisms rather than proving a direct synergistic interaction at the cellular level. Collectively, these effects suggest that during this period, microbial oxidation efficiency was compromised, thereby altering the redox balance and slowing the overall solubilization of metals.

$$Eh = E^{\circ\prime}_{Fe^{3+}/Fe^{2+}} + \frac{RT}{F} ln(\frac{aFe^{3+}}{aFe^{2+}}) = E^{\circ\prime}_{Fe^{3+}/Fe^{2+}} + \frac{2.303RT}{F} log_{10}(\frac{Fe^{3+}}{Fe^{2+}}) \quad (3)$$

with n=1. At our experimental temperature T=35°C(=308.15 K), the Nernst slope is:

$$\frac{2.303RT}{F} = 61.15 \text{ mV decade}-1 \quad (4)$$

I replaced the qualitative statement with a regression using our measured Fe^{3+} and Fe^{2+} concentrations (UV–VIS), paired to contemporaneous Eh (converted from Ag/AgCl to SHE and temperature-corrected). As expected for a $1e^-$ couple at 35 °C, Eh scales linearly with $\log_{10}\left(\frac{Fe^{3+}}{Fe^{2+}}\right)$.

$$Eh=\alpha+\beta\log_{10}\left(\frac{Fe^{3+}}{Fe^{2+}}\right) \quad (5)$$

The fitted linear relationship between the measured redox potential (Eh) and the logarithmic Fe^{3+}/Fe^{2+} ratio exhibited a slope of $\beta = 0.061 \pm 0.002$ V decade^{-1} (at 35 °C), which is in excellent agreement with the theoretical Nernstian prediction of 61.15 mV decade^{-1} for a one-electron transfer at this temperature. The intercept, $\alpha = E^{o\prime}(Fe^{3+}/Fe^{2+}) = 0.686 \pm 0.015$ V vs. SHE, reflects the apparent standard potential under the experimental ionic strength of the leachate matrix. The coefficient of determination ($R^2 = 0.94$) confirms a strong linear correlation, and the residual analysis showed no systematic deviation, indicating that the Fe^{3+}/Fe^{2+} equilibrium effectively governed the solution redox potential across the entire concentration range studied.

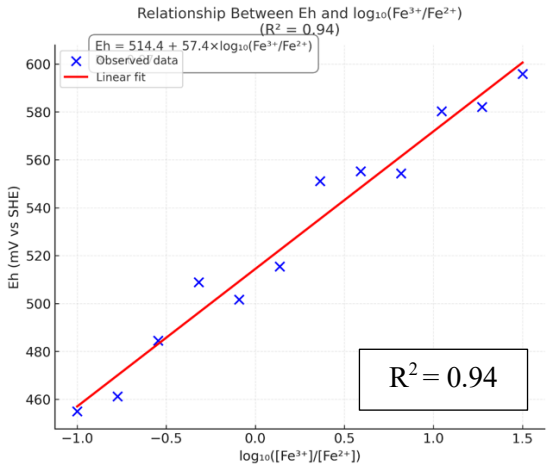

Fig. 13. Relations between Eh and $\log_{10}\left(\frac{Fe^{3+}}{Fe^{2+}}\right)$ in different initial Fe^{2+} concentration

3.2.2. Effect of pulp density

In all three bioleaching experiments, pulp densities of 5, 10, 15, and 20% (w/v) were employed, using feed material with particle sizes below 100 µm. A control test, carried out under identical conditions but without microbial inoculation (abiotic control), showed negligible dissolution of critical metals from the spent FCC catalyst. The investigation has shown the effect of pulp density on lanthanum, cerium, titanium and vanadium extractions from spent FCC catalyst where about 95.5% of lanthanum, 90.5% of cerium, 92.5% of titanium and 60.8% of vanadium were recovered in 7 days (Figure 14-17).

A control test conducted under identical experimental conditions but without microbial inoculation demonstrated only minimal dissolution of critical metals, yielding 1.1% for lanthanum, 0.5% for cerium, 1.5% for titanium, and 0.8% for vanadium. These values are significantly lower than those obtained in the bioleaching experiments, clearly indicating that abiotic leaching alone contributes negligibly to metal solubilization under the studied conditions. This comparison confirms that the dissolution of metals is predominantly driven by microbial activity rather than chemical leaching processes. Furthermore, the low recovery efficiencies observed in the abiotic control highlight the essential role of iron-oxidizing bacteria in sustaining the Fe^{3+}/Fe^{2+} redox cycle and generating the acidic and oxidative conditions necessary for effective metal mobilization.

During the bioleaching experiments, the ORP was primarily regulated by the redox cycling between ferric and ferrous ions. At the time of feed addition, redox potentials were approximately 350 mV for pulp densities of 5% and 10%, and around 340 mV for 15% and 20% pulp densities at 35°C (Fig. 19). A sharp decline in ORP was observed within the first two days, indicating that metal dissolution at this stage was largely driven by the combined action of ferric ions and protons. In the case of the 10% pulp density experiment, the dissolution trends of lanthanum, cerium, titanium, and vanadium point to the dominant contribution of microbially regenerated ferric ions. Maximum leaching of these metals was

achieved by the 8th day, which coincided with characteristic changes in pH, ORP, and ferrous ion concentrations that further support the occurrence of active biooxidation.

Subsequent trends in the 10% pulp density experiment showed a slight rise in ferrous ion concentration on the 9th day, accompanied by decreases in both pH and ORP. By the 13th day, a modest increase in ORP and pH, along with a reduction in ferrous ion levels, suggested a relatively low rate of microbial ferrous oxidation at this pulp density. Another factor contributing to the reduced involvement of ferric ions in the leaching process may be their precipitation. Evidence for this is provided by the continuous decline in ferrous ion concentration after day 9 in the 5% and 15% pulp density systems, and after day 8 in the 10% pulp density system, together with the consistently low ORP values that rule out any substantial Fe^{2+}/Fe^{3+} redox cycling. These findings emphasize the role of redox mediators in facilitating extracellular electron transfer (EET), which drives a cascade of microbial electro-catalytic reactions. Such mediators enable charge transport and govern the electrochemical pathways in biooxidation at the microorganism–substrate interface. A broad spectrum of redox transformations can occur through these mediators, accounting for the functional mechanisms underlying microbial electro-catalysis (Liu et al., 2018). Therefore, the possible involvement of such internal redox mediators is proposed here as a plausible hypothesis rather than a confirmed mechanism, pending further experimental verification.

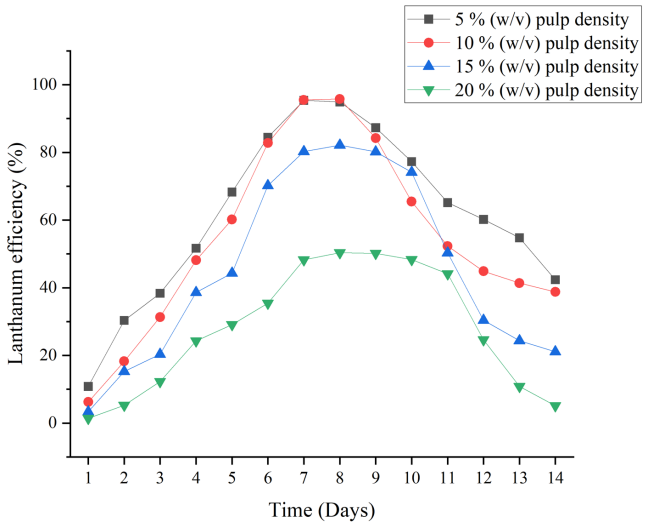

Fig. 14. Lanthanum bioleaching efficiency (%) by *Acidithiobacillus ferrooxidans* and *Leptospirillum ferrooxidans* at 5–20% pulp density

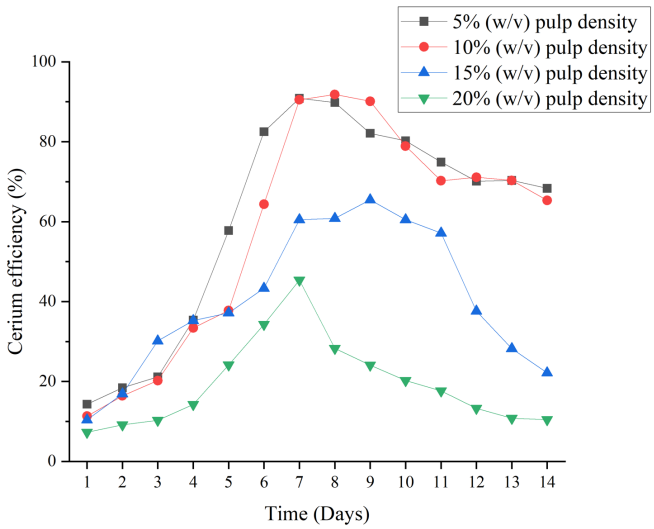

Fig. 15. Cerium bioleaching efficiency (%) by *Acidithiobacillus ferrooxidans* and *Leptospirillum ferrooxidans* at 5–20% pulp density

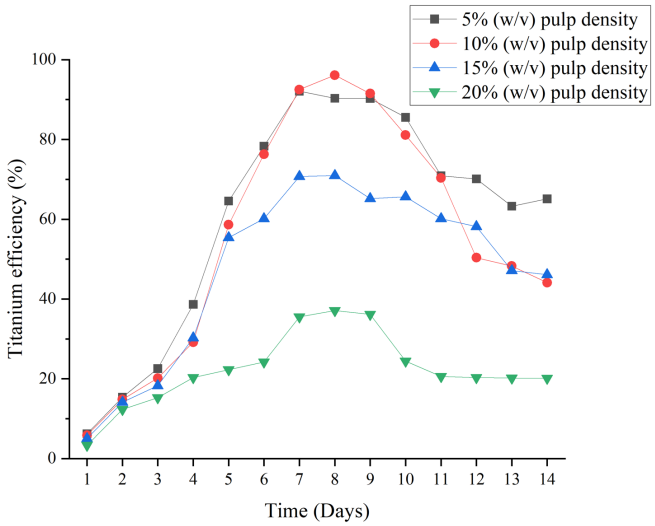

Fig. 16. Titanium bioleaching efficiency (%) by *Acidithiobacillus ferrooxidans* and *Leptospirillum ferrooxidans* at 5–20% pulp density

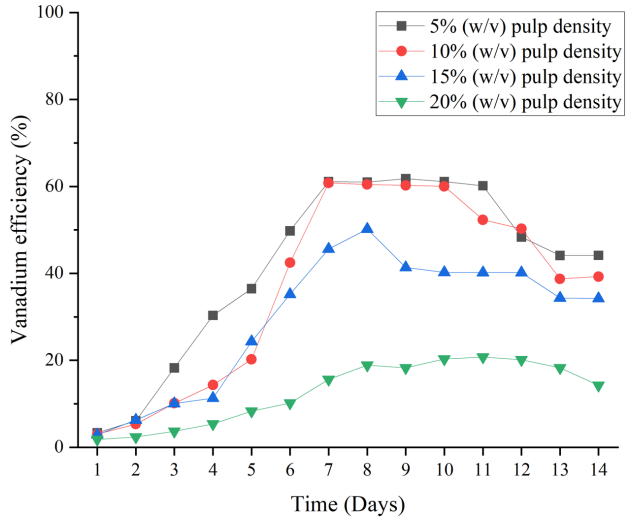

Fig. 17. Vanadium bioleaching efficiency (%) by *Acidithiobacillus ferrooxidans* and *Leptospirillum ferrooxidans* at 5–20% pulp density

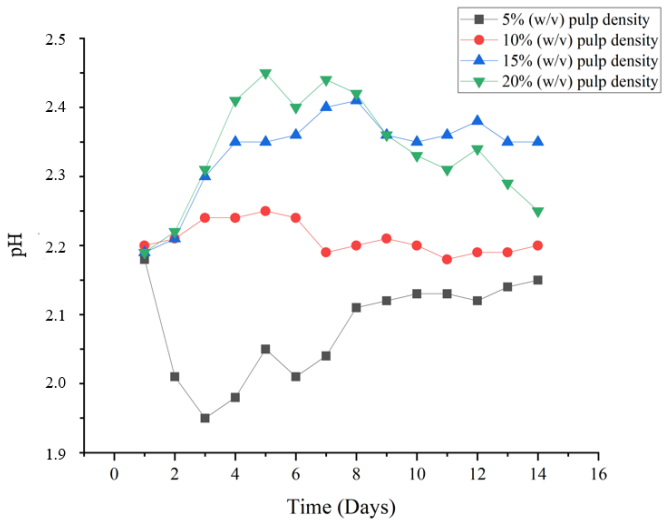

Fig. 18. pH variation during the bioleaching at different pulp densities

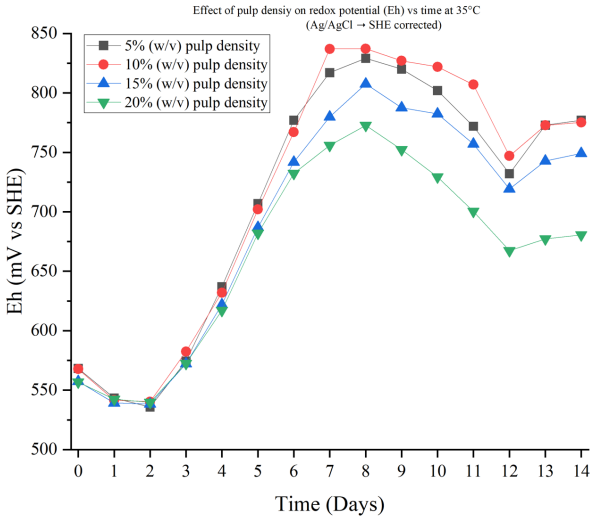

Fig. 19. Effect of pulp density on redox potential (Eh) during bioleaching at 35°C

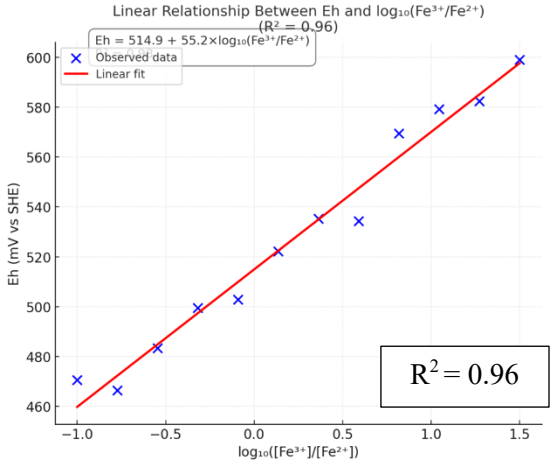

Fig. 20. Relations between Eh and $\log_{10}\left(\frac{Fe^{3+}}{Fe^{2+}}\right)$ in different pulp density

4. Conclusions

This study demonstrated the effectiveness of biohydrometallurgical methods for the recovery of critical metals – including lanthanum, cerium, titanium, and vanadium – from spent FCC catalysts. Characterization analyses (WD-XRF, XRD, SEM-EDS) confirmed the presence of significant quantities of these elements, particularly La_2O_3 (1.44%), TiO_2 (1.43%), and CeO_2 (0.23%), highlighting the potential of FCC waste as a valuable secondary resource.

The bioleaching experiments with *Acidithiobacillus ferrooxidans* and *Leptospirillum ferrooxidans* revealed that both initial ferrous ion concentration and pulp density strongly influence leaching efficiency. The results indicate that the dual-bacteria system is a promising strategy for maintaining redox-active bioleaching conditions and achieving efficient recovery of REEs and associated critical metals from spent FCC catalysts. Optimal conditions were obtained at 5 g/L Fe^{2+} and 10% pulp density, where recovery reached 95.5% for La, 90.5% for Ce, 92.5% for Ti, and 60.8% for V within seven days. Beyond this period, efficiency decreased due to jarosite formation and microbial activity limitations, underscoring the importance of controlled redox and pH conditions.

Overall, the results confirm that bioleaching offers a sustainable and efficient alternative to conventional chemical leaching for recovering critical metals from petroleum refinery waste. The process not only aligns with circular economy principles by minimizing reliance on virgin rare earth extraction but also addresses environmental challenges associated with spent catalyst disposal. Future

work should focus on scaling up the bioleaching process, optimizing microbial consortia, and integrating downstream separation methods to enhance recovery efficiency and economic feasibility.

Acknowledgments

The author gratefully acknowledges the financial support of the Ministry of Industry and Technology of the Republic of Türkiye through the "Enhancing Turkey's Research and Innovation Capacity for Rare Earth Elements Project" (REE Project). Appreciation is also extended to the R&D Department of the Turkish Oil Refineries Corporation, Türkiye, for kindly providing the spent catalyst samples used in this research.

References

AKCIL, A., VEGLI`O, F., FERELLA, F., OKUDAN, M.D., TUNCUK, A., 2015. *A review of metal recovery from spent petroleum catalysts and ash.* Waste Manag. 45, 420–433.

AKHTAR, M.S., ALI, S., ZAMAN, W., 2024. *Recent Advancements in Catalysts for Petroleum Refining*. Catalysts, 14(12), 841.

AUNG, K.K.M., TING, Y-P., 2005. Bioleaching of spent fluid catalytic cracking catalyst using Aspergillus niger. Journal of Biotechnology 116, 159–170.

BAYRAKTAR, O., 2005. *Bioleaching of nickel from equilibrium fluid catalytic cracking catalysts.* World J Microbiol Biotechnol 21, 661–665.

BOON M., HEIJNEN J., 1998. *Chemical oxidation kinetics of pyrite in bioleaching processes*. Hydrometallurgy 48, 27–41.

DAOUD, J. KARAMANEV, D., 2006. *Formation of jarosite during Fe^{2+} oxidation by Acidithiobacillus ferrooxidans*. Minerals Engineering, 19 (9), 960-967.

DAS, S., DESHAVATH, N.N., GOUD, V.V., DASU, V., 2019. *Bioleaching of Al from spent fluid catalytic cracking catalyst using Aspergillus species*. Biotechnology Reports, 23, e00349.

FERELLA, F., INNOCENZI, V., MAGGIORE, F., 2016. *Oil refining spent catalysts: a review of possible recycling technologies*. Resour. Conserv. Recycl. 108, 10–20.

FERELLA, F., D'ADAMO, I., LEONE, S., INNOCENZI, V., DE MICHELIS, I., VEGLIÒ, F., 2019. *Spent FCC E-Cat: Towards a Circular Approach in the Oil Refining Industry*. Sustainability, 11(1), 113.

KANNAN, S.G., FLEMING, M., HIRWA, J., CASTILLO, E., EGGERT, R., 2025. *Critical materials and manufacturing: Comparing China, the European Union, Japan, and the United States*. Resources, Conservation & Recycling Advances, 25, 2025, 200250,

LI, P. P., PENG, C. S., LI, F. M., SONG, S. X., JUAN, A. O., 2011. *Copper and nickel recovery from electroplating sludge by the process of acid-leaching and electro-depositing*. International Journal of Environmental Research, 5, 797–804.

LIU, X., SHI, L., GU, J.D., 2018. *Microbial electrocatalysis: redox mediators responsible for extracellular electron transfer*. Biotechnol Adv, 36(7), 1815–1827.

MOUSAVI, S.M., YAGHMAEI, S., VOSSOUGHI, M., ROOSTAAZAD, R., JAFARI, A., EBRAHIMI, M., HABIBOLLAHNIA CHABOK, O., TURUNEN, I., 2008. *The effects of Fe(II) and Fe(III) concentration and initial pH on microbial leaching of low-grade sphalerite ore in a column reactor*. Bioresource Technology, 99 (8), 2840-2845.

MOUNA, H.M., BARAL, S. S., MOHAPATRA, P., 2021. *Leaching of metals from spent fluid catalytic cracking catalyst using Acidothiobacillus ferrooxidans and comparing its leaching efficiency with organic and inorganic acids.* Journal of Environmental Chemical Engineering, 9 (5), 105522.

MUDDANNA, M.H., BARAL, S.S., 2019. *A comparative study of the extraction of metals from the spent fluid catalytic cracking catalyst using chemical leaching and bioleaching by Aspergillus niger*. Journal of Environmental Chemical Engineering, 7(5), 103335.

NAGAR N., GARG H., SHARMA N., AWE S.A., GAHAN C.S., 2021. *Effect of pulp density on the bioleaching of metals from petroleum refinery spent catalyst*. 3 Biotech. 11(3), 143.

SANTHIYA, D., TING, Y.P., 2006. *Use of adapted Aspergillus niger in the bioleaching of spent refinery processing catalyst*. J. Biotechnol. 121, 62–74,

SILVERMAN, M.P., LUNDGREN, D.G., 1959. *Studies on the chemoautotrophic iron bacterium. Ferrobacillus ferrooxidans, I. An improved medium and a harvesting procedure for securing high cell yields.* Journal of Bacteriology 77 (5), 642-647.

SRICHANDAN, H., MOHAPATRA, R.K., PARHI, P.K. MISHRA, S., 2019. *Bioleaching approach for extraction of metal values from secondary solid wastes: a critical review.* Hydrometallurgy 189, 105122.

SUGANUMA, S. KATADA, N., 2020. Innovation of catalytic technology for upgrading of crude oil in petroleum refinery. Fuel Process. Technol. 2020, 208, 106518.

WANG, YJ., LI, LL., ZHAO, S. Yu, A-F., 2023. *Bioleaching of metals from spent fluid catalytic cracking catalyst using adapted Acidithiobacillus caldus.* Environ Sci Pollut Res 30, 125689–125701.

ZHANG, S., XIN, B., 2025. *Rapid Regeneration of Spent FCC Catalysts through Selective Bioleaching by the Spent Medium Process*. ACS Omega, 10 (15), 15563−15571.